Identification of Form III Conformers in tRNA^{Phe} from *Escherichia coli* by Intramolecular Photo-Cross-Linking†

Yolande Lemaigre Dubreuil, Lamine Kaba,‡ Eliane Hajnsdorf, and Alain Favre*

Laboratoire de Photobiologie Moléculaire, Institut Jacques Monod, Université Paris VII, Tour 43, 2 Place Jussieu, 75251 Paris Cedex 05, France

Received February 6, 1986; Revised Manuscript Received May 15, 1986

Appendix: Computation of the Radius of Gyration of a Closed Ring to Which Linear Side Chains Are Attached

Marc Le Bret

Laboratoire de Physicochimie Macromoléculaire, Institut Gustave Roussy, 94800 Villejuif, France

ABSTRACT: In the absence of divalent cations, at neutral pH, low ionic strength, and low to moderate temperature, tRNAs are known to be in a denatured form, designated form III in the tRNA phase diagram by Cole et al. [Cole, P. E., Yang, S. R., & Crothers, D. M. (1972) *Biochemistry 11*, 4358–4368]. Form III tRNA^{Phe} from *Escherichia coli* has been studied at pH 7, 5 mM Na^+, and 10 °C. As judged from ethidium bromide intercalation, it exhibits extensive secondary structure. 4-Thiouridine in position 8 of the tRNA^{Phe} sequence was used as a built-in photoaffinity probe. Spectroscopic and spectrofluorometric analysis in the near-UV range of form III tRNA^{Phe} irradiated with broad-band near-UV light to completion of the reaction before or after reduction with $NaBH_4$ revealed that the Pdo(4–5)Cyt (8-C) and Pdo(4–5)Urd (8-U) adducts form in equimolar yield. In different experiments, the overall yield of s^4U conversion to these adducts varies between 20 and 40%. The remaining s^4U is photolyzed to weakly absorbing product(s) in the near-UV range. The disappearance of s^4U follows biexponential kinetics while the 8-C adduct formation follows monoexponential kinetics, indicating the presence of at least two tRNA classes of conformers, not in equilibrium on the time scale of the reaction. Migration on a denaturing polyacrylamide gel of irradiated form III tRNA^{Phe} revealed three main bands, D_1, D_2, and D_3, and no slowly migrating tRNA dimers. D_1 migrates at the control position and presumably contains the photolysis product(s) P. The fast-migrating D_2 and D_3 bands contain 8-Pyr cross-links which were identified by sequence analysis as 8–(66–68) in D_2 and 8–(40–43) and 8–(59–62) in D_3. On the basis of these data, it is proposed that the minor poorly photoreactive class II conformers are the cloverleaf and close variants, whereas the major class I cross-linkable conformers are essentially long-extended secondary structures. Clearly, our data demonstrate the polymorphism of form III tRNA^{Phe}.

Natural ribonucleic acids have very complex conformational properties. For example, some transfer ribonucleic acid (tRNA)[1] species such as tRNA^{Trp} from *Escherichia coli* (Lindahl et al., 1966) and tRNA^{Leu} from yeast (Gartland & Sueoka, 1966) can exist under metastable "denatured" conformations from which biological activity can be recovered by heat treatment under appropriate ionic conditions. For most tRNA species, however, at pH values close to neutrality, the conformational states are essentially in a temperature and ionic environment dependent equilibrium (Riesner et al., 1969; Goldstein et al., 1972). Monitoring the conformational changes of *E. coli* tRNA, free of divalent cations, as a function of temperature and ionic strength, by means of the 330-nm absorbance of 4-thiouridine, led Cole et al. (1972) to define an equilibrium phase diagram for several tRNAs. The diagram was found to be qualitatively similar for tRNA species containing either small variable loops (tRNA^{fMet}, tRNA^{Phe}) or large variable loops (tRNA^{Tyr}). Four distinct conformational forms (or phases) of tRNA were proposed. Form I, obtained at high ionic strength and low to moderate temperature, corresponds closely to the tRNA native structure as subsequently established by NMR analysis [see reference and discussion in Hyde & Reid (1985a)]. Essential features of this form are very close to the tRNA L conformation analyzed by X-ray crystallography (Quigley et al., 1975; Ladner et al., 1975). Form IV corresponds to the highest range of temperature and can be approximately described as a random coil. Forms II and III are much less structurally defined. On the basis of low activation energy in the I–II conversion, this latter form was proposed to be a cloverleaf structure or close variant.

† This investigation was supported by Centre National de la Recherche Scientifique, Universités Paris VI et Paris VII, and Ligue Nationale de la Recherche contre le Cancer.

‡ Present address: Laboratoire de Physico-chimie des systèmes polyphasés, CNRS, Route de Mende, 34033 Montpellier Cedex, France.

[1] Abbreviations: tRNA, transfer ribonucleic acid; D, dihydrouridine; m^7G, 7-methylguanosine; Ψ, pseudouridine; s^4U, 4-thiouridine; poly(s^4UC), copolymer of s^4U and cytidine; Pyr, pyrimidine; NMR, nuclear magnetic resonance; RPC, reverse-phase chromatography; EDTA, ethylenediaminetetraacetic acid; SDS, sodium dodecyl sulfate; pN, nucleoside 5′-monophosphate; *A*, absorbance; PRS, phenylalanine-tRNA synthetase; ^{32}P, phosphorus-32; Tris, 2-amino-2-(hydroxymethyl)-1,3-propanediol; Pyo(4–5)Ura, pyrimidin-2-one(4–5)uracil; Pyo(4–5)hUra, pyrimidin-2-one(4–5)dihydrouracil; Pyo(4–5)Cyt, pyrimidin-2-one(4–5)-cytosine; Pyo(4–5)hCyt, pyrimidin-2-one(4–5)dihydrocytosine; Pdo(4–5)Cyd (or Urd), N_1N_1'-diribonucleoside of Pyo(4–5)Pyr; 8-C and 8-U, Pyo_8(4–5)Pyr.

0006-2960/86/0425-5726$01.50/0

Subsequent NMR studies of *E. coli* tRNA^{Phe} thermal denaturation, in the presence of a few Mg^{2+} equivalents, have confirmed that the tertiary structure unfolds first (Hyde & Reid, 1985b). As yet, the study of form III tRNA is not readily accessible to study by NMR since the nucleic acid concentration required leads to an ionic strength too high for this form to predominate. On the basis of its slow kinetics and high activation energy of conversion to form I, it was proposed that form III possesses alternative secondary structure(s) distinct from the cloverleaf (Cole et al., 1972).

To analyze further the conformation(s) of form III *E. coli* tRNA^{Phe}, we have used the built-in probe 4-thiouridine, s^4U, present exclusively in position 8 of the sequence. In all form I native *E. coli* tRNAs containing the s^4U_8 and C_{13} residues, 335-nm photoexcitation leads to the selective and quantitative formation of the 8–13 link (Favre et al., 1969, 1975a), indicating close juxtaposition of the 8 and 13 residues which are found stacked on each other in crystalline yeast tRNA^{Phe} (Ladner et al., 1975; Quigley et al., 1975). The possibility of exploring the alternative conformations of tRNA using this probe were raised by the following findings: (i) 4-thiouracil (or its N_1-substituted derivatives) is able to photoreact with uracil or cytosine to yield respectively Pyo(4–5)Ura and Pyo(4–5)Cyt (or the N_1N_1'-substituted analogues) (Bergstrom & Leonard, 1972a; Thomas et al., 1978), and (ii) when randomly incorporated into the single-strand chain poly(s^4U-C), the 4-thiouracil residues leads to the intramolecular formation of the Pyo(4–5)Cyt photoadduct with a conversion yield of s^4U into adduct close to 15% (Favre & Fourrey, 1974).

Here, we show that near-UV irradiation of tRNA^{Phe} at low ionic strength triggers the intramolecular formation, with appreciable yield, of the Pyo(4–5)Cyt and Pyo(4–5)Ura adducts. Some of the predominantly formed cross-linked positions were identified allowing a better description of form III tRNA.

Materials and Methods

Products. Total tRNA and tRNA^{Phe} from *E. coli* MRE 600 were from Boehringer Mannheim. P_1 nuclease and pancreatic RNase were from Calbiochem, T_1 RNase was from Sankyo, and T_4 polynucleotide kinase was from P-L Biochemicals. Ethidium bromide was from Boots and pure drug. Acrylamide and bis(acrylamide) were from Serva. Stains-all was from Eastman Kodak Co. All other products used were obtained from Merck. [γ-^{32}P]ATP was purchased from Amersham.

tRNA^{Phe} Purification. This was achieved by reverse-phase RPC 5 chromatography as described by Pearson et al. (1971). The column, 60 cm high and 1 cm diameter, was equilibrated with the 0.45 M NaCl–5 mM sodium acetate, pH 4, buffer. A total of 50 A_{260} units of commercial tRNA^{Phe} was applied and elution performed by means of a linear NaCl gradient (120 mL, 0.45–1.1 M). Three peaks were obtained that represent respectively 5%, 85%, and 10% of the finally recovered material. The first one corresponds to tRNA fragments, the second one corresponds to pure intact tRNA^{Phe}, and the third one corresponds to 8–13 cross-linked tRNA^{Phe} as judged from (i) the fluorometric assay described below and (ii) the elution position of a cross-linked tRNA sample. Intact tRNA^{Phe} was precipitated and lyophilized until used.

Divalent Cation Removal from tRNA. tRNA samples (40 A_{260} units dissolved in 5 mL of deionized and bidistilled water) were successively dialyzed 2 times at 4 °C for 4 h against a 0.15 M NaCl–20 mM EDTA–0.1 mM sodium cacodylate, pH 7, buffer. This was followed by three 2-h dialyses against a 0.1 mM sodium cacodylate, pH 7, buffer containing 5 mM NaCl (buffer I). The dialyzed samples (less than 1 Mg^{2+} remaining per molecule) were divided in aliquots of 5 A_{260} units and kept until used at −20 °C.

Physical Techniques. Absorption spectra were measured with a Cary 15 spectrophotometer. Fluorescence measurements were taken with a Jobin-Yvon spectrofluorometer. Illumination of the tRNA samples was performed with the Lantern Cunow System equipped with an HBO 200-W superpressure mercury lamp (OSRAM) and a MTO J 310a filter. Cuvettes (path length = 1 cm) were placed 5 cm from the exit slit of the lantern and held in a thermostated holder.

$NaBH_4$ Reduction. All tRNA samples were reduced with $NaBH_4$ under identical conditions. Typically, a 50-μL aliquot (0.25 A_{260} unit) was diluted in 500 μL of 5 mM NaCl–10 mM $MgCl_2$–0.1 mM sodium cacodylate, pH 7, renaturing buffer (buffer II). Reduction was initiated by adding to each sample 50 μL of 50 mM NH_4OH and 100 μL of a freshly prepared $NaBH_4$ solution (25 mM). It was performed overnight at 4 °C in the dark. Samples were then neutralized by adding 100 μL of 1 M sodium acetate, pH 4.5. The fluorescence was then read at 20 °C in 800-μL cuvettes.

Analysis of Data. The bicomponent analysis of the near-UV ($\lambda > 340$ nm) absorption spectra of irradiated reduced hydrolyzed tRNA^{Phe} was performed as described by Reid and Pratt (1960) and Guschlbauer et al. (1965) using a Data General Eclipse S/130 computer. For analysis of the kinetics data as a sum of exponential terms, the Provencher program (Provencher, 1976), kindly provided to us by F. Rodier, was applied by using a Univac 1110 computer.

Purification of tRNA^{Phe} by Gel Electrophoresis. Preparative denaturing polyacrylamide slab gel (260 × 150 × 1 mm) contained 7 M urea, 10% (w/v) acrylamide, and 0.3% (w/v) bis(acrylamide). It was prepared in the electrophoresis buffer 0.045 M Tris–borate, pH 8.3, and 1.25×10^{-3} M Na_2EDTA. The samples were resuspended in 0.045 M Tris–borate, pH 8.3, 1.25×10^{-3} M Na_2EDTA, 8 M urea, and 0.025% (w/v) of each of the two markers xylene cyanol and bromophenol blue (sample buffer) and loaded onto the gel which was run at 7 W for 3 h. The fractionated products were visualized by fluorescence extinction under a germicide UV light irradiation of the gel layered on a fluorescent poly(ethylenimine) slab. tRNAs were eluted overnight from the polyacrylamide gel at room temperature under soaking in 0.03% (w/v) SDS–0.1 M ammonium acetate, pH 4.5, and were precipitated with cold ethanol. The precipitated material was resuspended in the sample buffer, reloaded onto a denaturing 10% polyacrylamide gel, visualized, and eluted as before.

5′-Terminal Labeling and Separation of Oligonucleotides Present in Enzymic Digests of tRNA^{Phe}. tRNA^{Phe} samples, purified as described, were subjected to complete enzymic digestion by pancreatic or T_1 RNase. Conditions were those of Silberklang et al. (1979). The reaction was conducted in 20 μL and contained 0.01–0.1 A_{260} unit of tRNA, 0.05 M Tris-HCl, pH 8, and either pancreatic RNase (0.5 μg/μg of tRNA) or T_1 RNase (1 unit/μg of tRNA). Samples to be digested with T_1 RNase were first denatured by heating at 100 °C for 1 min and quick cooling on ice before adding enzyme. After 3 h of incubation at 37 °C, the samples were either directly used for in vitro labeling or lyophilized and stored at −20 °C until needed. The in vitro phosphorylation reaction (5 μL) contained 0.1–1 μg of the tRNA digested as described earlier, (15–50) × 10^{-3} M Tris-HCl, pH 8, 10^{-2} M $MgCl_2$, 10^{-2} M dithiothreitol, 10 μg/mL bovine serum albumin, 10% glycerol, (1–1.5) × 10^{-9} mol of [γ-^{32}P]ATP (20–50 Ci/mmol), and 2–4 units of T_4 polynucleotide kinase. The

reaction mixture was incubated for 30 min at 37 °C and lyophilized. Each sample was resuspended in 8 M urea–0.025% (w/v) xylene cyanol, and loaded onto a 20% or 25% polyacrylamide slab gel (350 × 400 × 0.4 mm) containing 8 M urea and prepared in the electrophoresis buffer 0.1 M Tris–borate, pH 8.3, and 0.25 × 10^{-4} M Na_2EDTA. The weight ratio acrylamide to bis(acrylamide) was 20:1. The gel was preelectrophoresed for 2 h at 1800 V and run at 5 W overnight until the bromophenol blue marker had migrated 30 cm from the origin. 5′-Terminal-labeled oligonucleotides were revealed by autoradiography, eluted as described before in the presence of 1 μg of carrier tRNA, and precipitated twice with cold ethanol.

Identification of the 5′-Terminal Nucleotide by Thin-Layer Chromatography. The precipitates of 5′-terminal-labeled oligonucleotides were resuspended in 5 μL of 0.05 M ammonium acetate, pH 5.4, which contained 1 μg of nuclease P_1/μg of carrier tRNA, and incubated for 5 h at 37 °C. Released 5′ nucleotides were analyzed by thin-layer chromatography. The enzymic digests were evaporated, resuspended in distilled water, and applied onto each of two (20 × 20 cm) cellulose thin-layer plates along with UV markers (0.1 A_{260} unit of each pN). The plates were run at room temperature in two solvent systems: concentrated HCl/2-propanol/H_2O (15/70/15 v/v/v) and isobutyric acid/concentrated NH_4OH/H_2O (66/1/33 v/v/v) until the solvent front was about 1 cm from the top of the plate. UV-absorbing markers were detected under a 254-nm emitting UV light, and radioactive 5′-terminal nucleotides were visualized by autoradiography.

Results

tRNA Phases and Formation of the Pyo(4–5)Cyt Photoadduct. In order to delineate the relationship between the tRNA conformational state and formation of the 8–13 link, we have taken advantage of the method of Favre and Yaniv (1971). The 8–13 link adduct, formed in native tRNA, can be detected with high sensitivity and accuracy by using its fluorescence after $NaBH_4$ reduction to yield Pyo(4–5)hCyt (Bergstrom & Leonard, 1972b; Favre et al., 1972; Thomas et al., 1978). Total and purified tRNA were freed from Mg^{2+} as described under Materials and Methods. At the final stage of their preparations tRNA samples are in buffer I. Each sample is brought to a defined ionic environment by adding concentrated NaCl or $MgCl_2$ at 25 °C. The temperature is then adjusted to the desired value for at least 10 min and the illumination started. Aliquots are taken during the illumination and processed as described under Materials and Methods. It should be observed that all aliquots are placed in the same ionic conditions (buffer II, 25 °C) before $NaBH_4$ addition. In the various conditions used, the kinetics remains pseudo first order. However, the half-time of the reaction increases by a factor of 2.5 in denatured tRNA as compared to the native tRNA half-time (τ = 10 min). For the plateau level determination, the illumination time is taken at 120 min. As shown in Figure 1, the level of fluorescence, F, varies dramatically with both temperature, T, and cation concentration in agreement with previous observations (Favre et al., 1971). Clearly, formation of the 8–13 link is impeded in denaturing conditions. It should be noticed that some photoadduct forms in intact denatured tRNA while its formation cannot be detected with a T_1 RNase digest at the same concentration (data not shown). We have compared the F values in conditions which are characteristic of the different $tRNA^{Phe}$ forms as defined by Cole et al. (1972) and extended these measurements to total tRNA. As shown in Table I, the two samples exhibit very close behavior with a significant formation

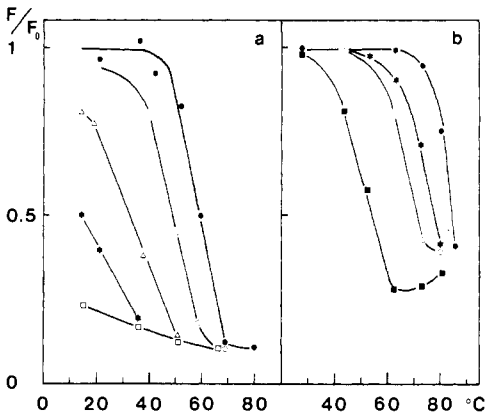

FIGURE 1: Formation of the Pyo(4–5)Cyt photoadduct in total tRNA as a function of the ionic environment and temperature conditions. Each tRNA aliquot freed from Mg^{2+} was brought at 25 °C to a defined ionic environment by addition of concentrated NaCl or $MgCl_2$ (final tRNA concentration 16 μM): (a) NaCl final concentrations: (●) 1, (○) 6 × 10^{-1}, (△) 2 × 10^{-1}, (asterisk) 2 × 10^{-2}, and (□) 5 × 10^{-3} M. (b) NaCl (5 × 10^{-3} M) and $MgCl_2$ final concentrations: (●) 5 × 10^{-3}, (asterisk) 10^{-3}, (○) 5 × 10^{-4}, and (■) 10^{-4} M. It was then equilibrated for 15 min at the appropriate temperature and illuminated for 120 min, and the fluorescence after $NaBH_4$ reduction, F (excitation λ_{max} 390 nm; emission λ_{max} 450 nm), was determined as described under Materials and Methods and Results. The data are expressed as the ratio F/F_0, F_0 being the reference value obtained with native tRNA.

Table I: Formation of the Pyo(4–5)Cyt Adduct in the Various Forms of tRNA[a]

T (°C)	20	50	10	60
Na^+ (mM)	176	176	5	5
bulk tRNA (%)	92 ± 3	12 ± 3	26 ± 3	8 ± 3
$tRNA^{Phe}$ (%)	100 ± 4	11 ± 2	25 ± 3	4 ± 1
phases	I	II	III	IV

[a] The Mg^{2+} free tRNA samples (Materials and Methods) were adjusted to the final temperature and cation concentration as described under Results. The final concentrations were respectively 8 (total tRNA) and 7 μM ($tRNA^{Phe}$). After illumination to the plateau level (120 min), all samples were reduced with $NaBH_4$ and neutralized, and the fluorescence F was read at 20 °C. Native tRNA samples irradiated in buffer II were used as reference (F_0 = 1). The data reported here are the ratios (F/F_0) × 100 obtained from two independent experiments.

of the photoadduct in conditions favoring form III tRNA. The dependence of F upon T for $tRNA^{Phe}$ is found similar to the one shown for total tRNA in Figure 1.

The data of Cole et al. (1972) indicate that form III retains a high degree of secondary structure. We have examined this property both on $tRNA^{Phe}$ and on total tRNA. The tRNA samples (1 μM) placed in buffer I are titrated with the dye ethidium bromide. This dye exhibits an enhanced fluorescence when intercalated into complementary double-stranded regions of both deoxyribonucleic and ribonucleic acids (Le Pecq et al., 1967; Favre et al., 1975b). The data (not shown) indicate that for the two samples, the number of intercalation sites per molecule is close to five in the denatured form instead of two to three in the native form (10 mM Mg^{2+}).

Spectroscopic Characterization of the 8-Pyr Photoadducts Obtained in Form III tRNA. The near-UV absorption spectra of native and form III $tRNA^{Phe}$ after illumination to the plateau level and (eventually) $NaBH_4$ reduction are shown in Figure 2. Native $tRNA^{Phe}$ behaves (Figure 2, insert) as already shown for different purified native tRNA species (Favre et al., 1971; Ofengand & Bierbaum, 1973). In contrast, immediately after near-UV irradiation of form III $tRNA^{Phe}$ there is a pronounced loss of absorbance at 330 nm. After $NaBH_4$ reduction a new broad near-UV-absorbing band ap-

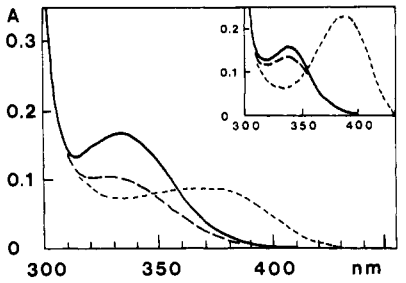

FIGURE 2: Absorption spectra of tRNA^{Phe} (14 μM) in the denatured form (buffer I) (—), after irradiation for 120 min (buffer I) (– –), and after $NaBH_4$ reduction in buffer II (- - -). The insert represents the same spectra obtained with native tRNA^{Phe} (14 μM) in 1 mM sodium cacodylate, pH 7, 0.1 M Na^+, and 10^{-2} M Mg^{2+}, before and after irradiation, and in buffer II after the subsequent reduction.

Table II: Near-UV Absorbance Characteristics of the Pyo(4–5)Pyr and Pyo(4–5)hPyr Reference Compounds at Neutral pH as a Function of the Substituents at the N_1N_1' Positions

	Pyo(4–5)Pyr		Pyo(4–5)hPyr	
	λ_{max} (nm)	ϵ (M^{-1} cm^{-1})	λ_{max} (nm)	ϵ (M^{-1} cm^{-1})
Pyr = Cyt				
unsubstituted	323	12 000[a]	374	24 300[d]
	323	13 700[c]		
N_1N_1'-dimethyl	330	16 000[b]	379	23 000[b,f]
N_1N_1'-diriboside	328	17 600[a,e]	379	23 300[e,f]
Pyr = Ura				
unsubstituted	[g]	[g]	355	17 600[d]
N_1N_1'-dimethyl	324	~18 000[f]	363	18 000[f]

[a] Rhoades & Wang (1971). [b] Thomas et al. (1978). [c] Bergstrom & Leonard (1972a). [d] Bergstrom & Leonard (1972b). [e] Favre et al. (1972). [f] unpublished results of J. L. Fourrey and A. Favre. [g] Unknown.

pears (Figure 2) which clearly cannot be due to the Pyo(4–5)hCyt adduct exclusively. The presence of this adduct is nevertheless demonstrated by its excitation and emission fluorescence spectra (not shown) which appear identical in shape to that of a control native tRNA, the apparent excitation λ_{max}, and emission λ_{max} being respectively 397 and 450 nm (Favre & Yaniv, 1971; Thomas et al., 1978). Assuming the absorbance at 390 nm, the standard excitation wavelength, to be exclusively due to the Pyo(4–5)hCyt adduct, it results an apparent quantum yield, Φ_{ap}, lower than Φ_0, the value obtained under similar conditions for native tRNA, $\Phi_{ap}/\Phi_0 = 40 \pm 3\%$.

The nature of the reduced adduct absorbing in the intermediate near-UV range (Figure 2) can be inferred from the known photochemical properties of 4-thiouracil which photoreacts readily with uracil to yield Pyo(4–5)Ura (Bergstrom & Leonard, 1972a; Thomas et al., 1978). This adduct and its N_1N_1'-substituted derivatives absorb at 335 nm and yield, upon $NaBH_4$ reduction, the Pyo(4–5)hUra (and derivatives), the absorption λ_{max} of which is between 355 and 363 nm (Table II). The absorbance spectra of irradiated form III tRNA^{Phe} after irradiation or irradiation and reduction (Figure 2) fits qualitatively well with a mixed formation of the Pyo(4–5)Cyt and Pyo(4–5)Ura photoadducts, abbreviated 8-C and 8-U in the following. The Pyo(4–5)hUra adduct and its derivatives are not known to fluoresce (Bergstrom & Leonard, 1972b; Thomas et al., 1978) in agreement with the spectrofluorometric data described earlier.

In order to determine precisely the respective amount of 8-C and 8-U adduct, a tRNA^{Phe} sample is irradiated to the plateau level, $NaBH_4$ reduced, and then digested to completeness. The near-UV absorption spectra (Figure 3) is then analyzed with respect to those of the reference compounds shown in Figure

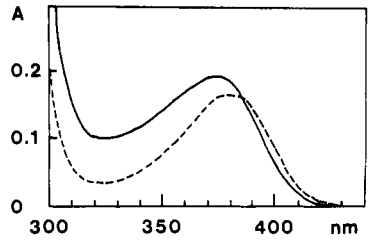

FIGURE 3: Near-UV absorption spectra of the enzymatic digest of irradiated $NaBH_4$ reduced form III tRNA^{Phe} (23 μM) (—) and form I tRNA^{Phe} (10.5 μM) (- - -). Digestion was performed overnight with 25 units of T_1 RNase, 50 units of pancreatic RNase, and 4 units of T_2 RNase.

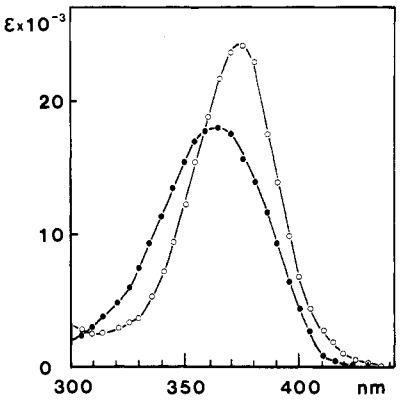

FIGURE 4: Absorption spectra of the reference model compounds. The molar extinction coefficient, ϵ, is expressed in M^{-1} cm^{-1}. N_1N_1'-Dimethyl-Pyo(4–5)hUra (●) and N_1N_1'-diriboside Pyo(4–5)hCyt (○).

Table III: Multicomponent Analysis of the Near-UV Absorption Spectra of Irradiated Reduced tRNA^{Phe} [a]

	8-C (%)	8-U (%)
A	98.5	1.5
B	48 ± 4	52 ± 4
C	55 ± 15	45 ± 15

[a] The absorption spectrum of tRNA^{Phe} irradiated, reduced, and digested to completion by nucleases was subjected to multicomponent analysis between 340 and 450 nm. The spectra of the reference compounds are shown in Figure 2. The data are presented as the percent contribution of each reference compound to the final spectra of (A) native tRNA^{Phe}, (B) form III tRNA^{Phe} irradiated to the plateau level, and (C) form III tRNA^{Phe} irradiated for 10 min, i.e., 50% s^4U photolysis. It was verified that taking into account the end absorption of normal tRNA bases using the spectrum of 4-thiouridine free tRNA (Thomas & Favre, 1977) does not significantly affect the analysis above.

4. These compounds were selected because they present the closest structural analogies with the potential reduced adducts of interest. In addition, it can be seen in Table II that the absorption characteristics of the adducts are very close whether the substituents at the N_1N_1' positions are ribose or methyl groups. Multicomponent analysis, as described by Reid and Pratt (1960) and Guschlbauer et al. (1965), is applied between 340 and 450 nm (see Materials and Methods). As shown in Table III, the two adducts are formed in equimolar amounts. The final concentration C of these adducts can be obtained by applying the Beer–Lambert law to the absorption spectra of Figure 3. For example at 380 nm

$$0.18 = (14\,400 + 23\,400)C$$

yielding a final conversion yield $C/C_0 = 20\%$, where C_0 is the initial s^4U concentration (23.5 μM). Hence, in this experiment, 40% of the initial s^4U is converted into adducts, the remaining 60% being photolyzed to an unknown product(s) P which, at most, weakly absorbs (absorb) light of wavelength longer than

Table IV: Decomposition of $F_1(t)$ and $F_2(t)$ as a Sum of Exponential Terms[a]

expt	$\lambda_1 \times 10^2$	$\lambda_2 \times 10^2$	a	b	c	$k_2 \times 10^2$	$k_3 \times 10^2$
1	6.1 (14%)[b] 7.9 (11%)[c]	1.2 (35%)	0.684 (14%)	0.233 (35%)	0.079 (5%)[d]	4.70	1.15
2	7.8 (17%)[b] 9.7 (12%)[c]	2 (63%)	0.738 (23%)	0.208 (80%)	0.053 (6%)[d]	7.14	0.93
3	6 (5%)[b] 6 (5%)[c]	1.2 (35%)	0.637 (12%)	0.254 (37%)	0.108 (6%)[d]	3.32	1.34

[a] The experimental values of $F_1(t)$ and $F_2(t)$, as defined under Results, were normalized to $F_1(0) = 1$. Treatment of the data by Provencher's method indicates that $F_1(t)$ and $F_2(t)$ can best be described by $F_1(t) = ae^{-\lambda_1 t} + be^{-\lambda_2 t} + c$ and $F_2(t) = c(1 - e^{-\lambda_1 t})$ with the rate constants λ_1 and λ_2 (min^{-1}) listed above. Footnote *b* refers to the data obtained with $F_1(t)$ and footnote *c* to $F_2(t)$. Values in parentheses are relative errors. Since the same coefficient c was obtained from $F_1(t)$ or $F_2(t)$, only the largest relative error was mentioned (footnote *d*). Rate constants k_2 and k_3 refer to the kinetic model analyzed under Discussion, assuming $\Phi/\Phi_0 = 0.65$. For comparison, the data obtained from form I $tRNA^{Phe}$ gives only one constant: $\lambda_1 = 14 \times 10^{-2}$ (6%) min^{-1}.

320 nm. The same treatment as above, applied to form I $tRNA^{Phe}$, indicates that the 8-C adduct contributes more than 98.5% (Table III) to the final absorption spectra, with a final conversion yield higher than 95%. Due to the hypochromic effects, it is not possible to accurately estimate the respective contributions of the reduced 8-U and 8-C adducts to the absorption spectra of undegraded irradiated $tRNA^{Phe}$. Assuming identical hypochromicities at the standard excitation wavelength, 390 nm, the actual yield of fluorescence emission, Φ, can be obtained after correction for the reduced 8-U absorbance by using the data of Figure 4. Hence

$$\Phi/\Phi_0 = (\Phi_{ap}/\Phi_0)(14\,000 + 9400)/14\,000 = 0.65$$

Certainly, Φ/Φ_0 is between 0.5 and 0.8.

Photochemical Kinetics in Form III $tRNA^{Phe}$. An accurate description of the events occurring during illumination of form III $tRNA^{Phe}$ requires the knowledge at any time of C_1, C_2, C_3, and C_4, the respective concentration of remaining s^4U, product(s) P, 8-C adduct, and 8-U adduct. In order to accurately follow the kinetics of s^4U consumption and 8-C adduct formation, $tRNA^{Phe}$ (5 A_{260}) in buffer I was illuminated at 10 °C. Two irradiated samples were taken at time t and treated in parallel. Sample 1 was renatured by addition of Mg^{2+} to a final concentration of 10 mM (controls indicate that renaturation is quantitative as judged by 8–13 link formation) and reilluminated to the plateau level. The two samples (1 and 2) were then placed in buffer II, reduced, and processed as described under Materials and Methods. This procedure yields two fluorescence signals per t value, $F_1(t)$ and $F_2(t)$, and the result of a typical experiment is shown in Figure 5. Clearly, $F_2(t)$ is a measure of the 8-C link formed and is related to the adduct concentration, C_3 (K being a constant), by

$$F_2(t) = K\Phi C_3$$

If the fluorescence measurements are expressed in arbitrary units and, accordingly, $F_1(0) = K\Phi_0 C_0$ is used as a normalizing factor $F_1(0) = 1$, then

$$F_1(t) = K(\Phi_0 C_1 + \Phi C_3)$$

and when these equations are combined

$$C_3/C_0 = F_2(t)\Phi_0/\Phi$$

$$C_1/C_0 = F_1(t) - F_2(t)$$

The latter expression is in agreement with the observation (Figure 5) that at the plateau level $F_2(\infty) = F_1(\infty)$ meaning that all s^4U has been consumed, $C_1(\infty) = 0$.

Since illumination has been performed in conditions where the absorbance in the near-UV range remains less than 0.1, the kinetics are expected to be first order as indeed observed for form I $tRNA^{Phe}$. The $F_1(t)$ and $F_2(t)$ data were therefore analyzed by using the procedure of Provencher that yields the minimal number of exponential terms fitting the experimental

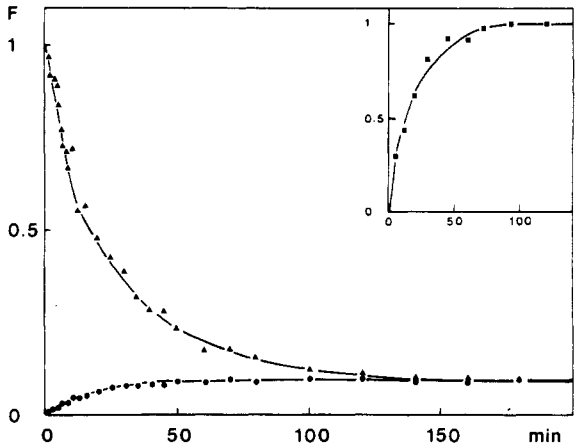

FIGURE 5: Kinetics of 8-C link formation and s^4U decay in illuminated form III $tRNA^{Phe}$. The $tRNA^{Phe}$ sample (5 μM) was illuminated at 10 °C in buffer I with broad-band near-UV light. At each indicated time, t, two aliquots (50 μL) were taken and diluted in buffer II (500 μL). One of them was subsequently reirradiated with near-UV light to the plateau level (120 min). After $NaBH_4$ reduction and neutralization, one obtains $F_1(t)$ (▲) and $F_2(t)$ (●). The insert shows, by comparison, the kinetics of 8–13 link formation in form I $tRNA^{Phe}$ (irradiation was performed at 10 °C in buffer II).

values (Provencher, 1976). It can be observed (Table IV) that, within experimental errors, the fastest rate constants are the same in $F_1(t)$ and $F_2(t)$. Hence

$$F_1(t) = ae^{-\lambda_1 t} + be^{-\lambda_2 t} + c$$

with $F_1(0) = a + b + c = 1$ and

$$F_2(t) = c(1 - e^{-\lambda_1 t})$$

C_3 and C_1 can now be written in the forms

$$C_3 = C_0 c(1 - e^{-\lambda_1 t})\Phi_0/\Phi$$

$$C_1 = C_0[(a + c)e^{-\lambda_1 t} + be^{-\lambda_2 t}]$$

From the coefficients listed in Table IV it is clear that although s^4U decays with a biexponential kinetics, the 8-C adduct is formed with an apparent first-order kinetics.

Separation of $tRNA^{Phe}$ Isoforms. We have compared the migration profiles of (A) native tRNA, (B) 8–13 cross-linked tRNA, (C) form III tRNA, and (D) illuminated form III tRNA obtained by electrophoresis on denaturing polyacrylamide gel (Figure 6). As expected, samples A and C have the same electrophoretic mobility while sample B migrates faster. Since samples A and B keep the same global charge, this behavior is interpreted as reflecting a decreased friction coefficient of the 8–13 cross-linked molecule in the presence of 7 M urea. Illuminated denatured tRNA, sample D, yields a more complex migration profile: three major bands D_1, D_2, and D_3 are reproducibly obtained in five independent experiments. No band can be detected that migrates at a slower

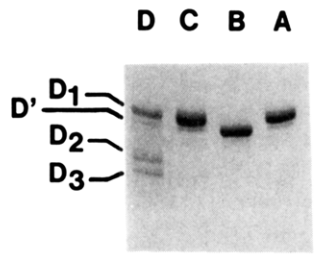

FIGURE 6: Electrophoretic pattern of tRNA^{Phe} on 10% polyacrylamide denaturing gel. The samples were loaded on the gel as (A) native tRNA^{Phe}, (B) 8–13 cross-linked tRNA^{Phe}, (C) form III tRNA^{Phe}, and (D) irradiated form III tRNA^{Phe}.

rate than the control A and C samples.

The result above indicates that (i) no intermolecular cross-link occurs in our illumination conditions and (ii) new fast-migrating conformers (D_2 and D_3) appear. In the presence of 7 M urea, the radius of gyration of these forms is even lower than that of sample B, which necessarily reflects their stabilization by an intramolecular covalent link between position 8 and another pyrimidine in position X in the sequence (link 8-X). The above result also indicates that (iii) the very minor band D′ is presumably due to a low level of 8–13 cross-linked tRNA contaminating all samples.

Identification of Cross-Linked Oligonucleotides in the Major (D) Conformers. The material from each band A–D_3 was purified and digested by T_1 or pancreatic RNases. The oligonucleotides were end labeled at their 5′ extremity with [γ-^{32}P]ATP, separated by gel electrophoresis, and visualized by autoradiography. Oligonucleotides were eluted and their 5′ end identified after P_1 nuclease digestion, thin-layer chromatography and autoradiography (see Materials and Methods). We focused our analysis onto oligonucleotides which are clearly distinct in the D and A or C conformers and reproducibly obtained in independent experiments.

As expected, samples A and C have the same electrophoretic pattern. When the size of the oligonucleotides, deduced from their electrophoretic mobility and their 5′-end analysis, is taken into account their attribution is shown in Figure 7. Sample B yields a new 9-mer with 5′ ends pA and pC which obviously result from the 8–13 cross-link (Figure 7). The 5-mer $CUC_{13}AG$ is clearly missing. The disappearance of the 4-mer As^{4}UAG is not apparent due to the poor resolution of the five 4-mers on the gel.

The pattern of sample D_1 is exactly the same as those of samples A and C and provides no indication for an intramolecular 8-Pyr cross-link. On the other hand, some new fragments are specifically and repetitively observed: Y_1 in sample D_2 and Y_2, Y_3, and Y_4 in sample D_3 (Figure 7). Y_1 migrates as an 8-mer just below the Um^{7}GXCCUUG. It results from the cross-link of the tetranucleotide As^{4}UAG with a 4-mer. The latter was identified as the tetranucleotide UCCG which can be resolved upon a 25% polyacrylamide gel of samples A, B, or C and which disappears in sample D_2 (data not shown). The autoradiography of cellulose plate on which the P_1 nuclease digest of Y_1 has been chromatographied reveals three radioactive spots: ^{32}pA, ^{32}pU, and a third one which remains close to the origin and is identified as a P_1-resistant dinucleotide pPdo(4–5)[^{32}P]pUrd. Hence, the 8-position can be covalently linked either to pU_{66} or to one of the cytidines at 67 or 68 (Figure 8). This is confirmed by the pancreatic RNase digest analysis which reveals a new 5-mer and a new 8-mer, indicating the cross-link of the s^{4}U containing pancreatic oligonucleotide, $GGAs^4U_8$ with either C in position 67 or 68, or the 4-mer $GAGU_{66}$ (data not shown). Y_2 has the mobility of the 13-mer T_1 oligonucleotide from tRNA^{Val}. Its ends

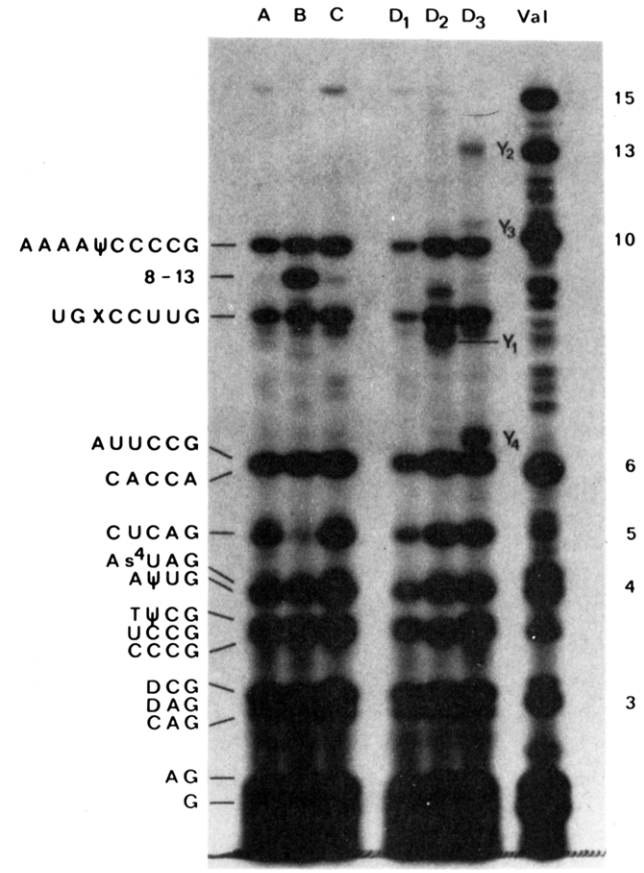

FIGURE 7: Autoradiography of the 5′-end-labeled T_1 oligonucleotides from different tRNA^{Phe} samples and from a control 8–13 cross-linked tRNA^{Val} after separation by electrophoresis on a 20% polyacrylamide denaturing gel. Samples A–C and D_1–D_3 were fractionated as in Figure 6 and repurified as described under Materials and Methods.

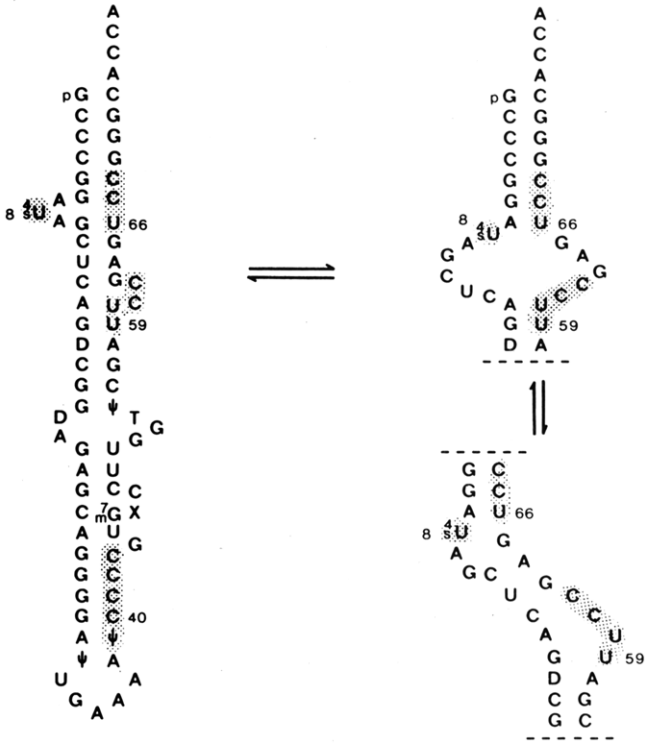

FIGURE 8: Extended secondary structures derived from the tRNA^{Phe} sequence by the procedure of Gouy et al. (1985).

analysis reveals only pA. Y_2 necessarily occurs from the cross-link between As^{4}UAG and the 10-mer. Hence, the 8-position is cross-linked to one of the cytidines at 40–43

(Figure 8). Y_3 migrates close to a 10-mer and exhibits only pA by ends analysis. It is likely that position 8 is actually cross-linked to one of the positions at 59–62 from the 6-mer. Y_4 migrates just above a 6-mer, and its ends analysis reveals only pA. On the basis of this limited information, it could not be further characterized.

Discussion

Formation of 8-C and 8-U Adducts in Form III tRNA^{Phe}. In contrast to the quantitative conversion of s^4U_8 into the 8–13 link observed in all form I tRNA species that contain s^4U_8 and C_{13} studied so far (Favre et al., 1975a), only a low yield of 8-C adduct is obtained in conditions where form III tRNA predominates (Figure 1 and Table I). This is in agreement with previous observations indicating little or no formation of this adduct in denatured tRNA (Favre et al., 1971; Ofengand & Bierbaum, 1973). A detailed spectrophotometric analysis of illuminated and illuminated $NaBH_4$-reduced tRNA^{Phe} shows that the 8-C and 8-U adducts form in equimolar amounts with a final yield close to 20%. Since all s^4U has been consumed at the end of the reaction, a photolysis product(s) designated P accumulates (accumulate) with a final yield of 60%. Although it is the major photoproduct obtained in form III tRNA^{Phe}, we know only that it weakly absorbs in the near-UV range. It should be noticed that, when illuminated in aqueous dilute solution, 4-thiouridine leads to a variety of photoproducts that only poorly absorb at wavelengths longer than 310 nm (Favre, 1974).

In this work, we have focused upon the 8-C and 8-U adducts since localization of these links contains potentially new structural information. In form III tRNA^{Phe}, s^4U_8 is able to photoreact with several distinct pyrimidines indicating, a priori, much more flexibility than observed in form I tRNA^{Phe}. Also the quantum yield, Φ, of emission of the $NaBH_4$-reduced 8-C residues is lower than Φ_0 when measured in the renaturing buffer, $\Phi/\Phi_0 \sim 0.65 \pm 0.15$. This indicates a surprisingly high microviscosity around the reduced 8-C adduct when form III tRNA^{Phe} is placed in buffer II (Thomas et al., 1978). Apart from form I tRNA^{Phe}, the only analogous system to which our data can be compared is random poly(s^4U-C) where intramolecular Pyo(4–5)Cyt links can be induced with a final yield of 15%. The quantum yield of Pyo(4–5)hCyt emission in this polynucleotide is only one-tenth that of native tRNA (Favre & Fourrey, 1974). A major difference between this random-coiled polynucleotide and form III tRNA^{Phe} is the presence of a high degree of secondary structure in the latter, as judged by ethidium bromide intercalation.

Different Conformers Are Present in Form III tRNA^{Phe}. This is obvious from the electrophoretic behavior of irradiated form III tRNA^{Phe} upon a denaturing gel (Figure 6). A first point that deserves attention is the lack of any band migrating at a slower rate than the control. Hence, we have no evidence for the formation, by *intermolecular* cross-linking, of tRNA dimers that could have been easily detected upon the gel. The ratio, ρ, of the initial rates of inter-cross-links, dP_1/dt, vs. intra-cross-links, dP_2/dt, can be assumed to be less than 1/100. ρ can be written as

$$\rho = (dP_1/dt)/(dP_2/dt) = (k_1/k_2)fC$$

where k_1 and k_2 are respectively bimolecular and unimolecular rate constants, f is an efficiency factor weighted by the respective fractions of s^4U available for inter- vs. intra-cross-linking, and C is the tRNA concentration (10^{-5} M). Since the unimolecular rate constant k_2 is in the range 10^{-3} s^{-1} (see below) and $\rho \leq 10^{-2}$, $k_1 f$ is lower than 1 M^{-1} s^{-1}. The upper limit for k_1 is k_q, the diffusional constant $k_q \approx 10^9$ M^{-1} s^{-1}. It is likely that both f and k_1 contribute to the absence of dimerization. Probably the predominant factor comes from strong electrostatic tRNA repulsions that would decrease the bimolecular rate constant by several orders of magnitude.

Figure 6 shows that irradiated form III tRNA^{Phe} yields three major bands, D_1, D_2, and D_3, over a weak smear. Sequence analysis provides clear-cut indication of the occurrence of 8-X cross-links in the fast-migrating D_2 (X = 66–68) and D_3 (X = 40–43 and 59–62) bands, although no cross-link could be detected in D_1 which migrates at the control position. Hence, it is clear that the D_1 conformer contains the photolysis product(s), P (possibly uridine), instead of 4-thiouridine although D_2 and D_3 are α-shaped molecules fixed by 8-U and/or 8-C cross-links. At neutral pH, both of these adducts are uncharged (Bergstrom & Leonard, 1972a; Favre et al., 1972; Thomas et al., 1978) so that the global charge of cross-linked tRNA remains unchanged. Hence, in the conditions of the gel, the friction coefficient necessarily decreases in the following order: intact tRNA^{Phe}, 8–13 linked tRNA^{Phe}, D_2, and D_3. This behavior can be easily understood if one assumes that tRNA molecules behave like random coils. A predominant factor determining the electrophoretic behavior should be their radius of gyration, R_G. For a random walk chain of N elements $R_G \sim (N/6)^{1/2}$ but decreases to $R_G \sim (N/12)^{1/2}$ for the same end to end closed chain. Hence, increasing the size loop should decrease R_G and increase the migration rate. The derivation of R_G for an α- or σ-shaped cross-linked random walk chain has been performed by M. Le Bret (see the Appendix). Also the R_G values of more realistic tRNA chains of defined thickness, either cross-linked or containing a knot, have been obtained by simulation (see Table V and Figure 9 in the Appendix). Clearly R_G is an important factor determining the tRNA mobility: X varies between 40 and 68 for the fast-migrating D_2 and D_3 forms. Yet, the 8–(40–43) cross-linked form migrates faster than expected on the basis of R_G only (Figure 6). Clearly, other factors are involved, possibly the presence of a local transient secondary structure or of a knot.

The gel migration behavior of α-shaped tRNA^{Phe} molecules is in contrast with most of the electrophoretic data obtained with α- or σ-RNAs of larger size (or their derived λ- and κ-branched structures). For example, the large loop containing psoralen cross-linked 16S RNA molecules exhibits the lower mobility upon a 5% formamide acrylamide gels (Wollenzien & Cantor, 1982). Similar data were obtained with 5S and PSTV RNA (Branch et al., 1985). Also in studying splicing intermediates, Grabowski et al. (1984) observed that α- or σ-shaped RNAs (or their derived λ and κ forms) exhibit anomalously high "apparent" molecular weight as compared to the parent linear molecule. The low relative mobility of the cross-linked forms furthermore increases with the gel concentration. This can be rationalized as follows: in the denaturing conditions of the gel a polynucleotide chain can be viewed as a mixture of conformers in fast equilibrium. When the gel pores have a mean diameter close to or lower than R_G, the migration of the different conformers will be strikingly affected. Extended conformations will be favored and will determine the overall sample behavior. In cross-linked or branched RNAs, these extended conformations are no more allowed, and the observed mobility decreases. Hence, the relative mobilities of the cross-linked α, σ, λ, or κ forms of a polynucleotide chain will in general be largely determined by the gel concentration and its degree of reticulation. Only when the gel pores are larger than R_G will this parameter be determinant to predict the RNA mobility.

Scheme I: Summary of 4-Thiouridine Photochemical Behavior in Form III and Form I tRNA^{Phe} [a]

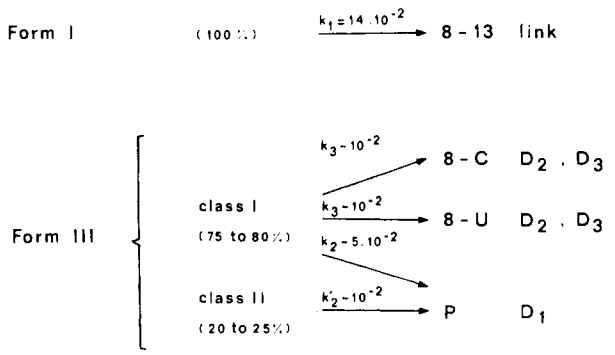

[a] Rate constants are expressed in min^{-1}.

Are the Conformers in Equilibrium? Formation of the 8–13 link in native tRNA^{Phe} under our conditions obeys apparent first-order kinetics (Table IV) as already observed before for other pure tRNAs (Favre et al., 1975a). This can be readily understood since (i) the reaction is intramolecular, and (ii) at the effective irradiation wavelengths, the absorption varies little and remains in any case lower than 0.1 in current experiments [see Ballini et al. (1976) for discussion]. This finding indicates that s^{4}U photoreacts at a constant rate on the time scale of the experiment (of the order of the minute), which can be taken as evidence either for a unique conformation or alternatively for multiple conformers with different reactivities but in fast equilibrium (compared to the time scale of the experiment). This latter view is supported by experiments in the presence of the cognate synthetase (PRS). Formation of the tRNA^{Phe}–PRS complex decreases, by a factor of 2.5, the rate of 8–13 cross-linking without affecting the s^{4}U triplet-state lifetime. These results have been interpreted as reflecting a selection by the enzyme of the less reactive "native" conformers (Favre et al., 1979).

The knowledge that intramolecular but not intermolecular photoreactions of s^{4}U occur (see above) as well as the fact that, in our illumination experiments, the absorbance at the wavelength of interest (300–400 nm) remains lower than 0.1 justifies our kinetic analysis. It reveals that although the 8-C formation can be adequately described by first-order kinetics of rate constant λ_1, the s^{4}U decay follows a more complex biexponential kinetics with rate constants λ_1 and λ_2. A full description of the s^{4}U photochemical behavior should involve the 8-U formation. Our limited data (Table III) agree with the finding that $C_3 \sim C_4$ at any time during the reaction (an alternative possibility that C_4 accumulates with the rate constant λ_2 would yield $4C_4 \sim C_3$ when $C_1 = C_0/2$ which is clearly unlikely). Hence, in the following we will assume $C_3 \sim C_4$ at any time during the reaction. This allows the derivation of C_2:

$$C_2/C_0 = 1 - (C_1 + 2C_3) = [a + c(1 - 2\Phi_0/\Phi)](1 - e^{-\lambda_1 t}) + b(1 - e^{-\lambda_2 t})$$

Clearly, when the experimentally determined coefficients are taken into account (Table IV), the accumulation of P follows biexponential kinetics.

The simplest model, accounting for this behavior, involves at least two conformational states, I and II, with state II leading exclusively to the formation of P (Scheme I). States I and II are proposed to equilibrate at a much slower rate than the photochemical rate constants. In these conditions, if f(I) and f(II), with f(I) + f(II) = 1, are the relative weighted concentrations of these states, then

$$C_1/C_0 = f(\mathrm{I})e^{-\lambda_1 t} + f(11)e^{-\lambda_2 t}$$

$$C_3/C_0 = f(\mathrm{I})(1 - e^{-\lambda_1 t})k_3/\lambda_1$$

By identification with previous expressions of C_1/C_0 and C_3/C_0

$$f(\mathrm{II}) = 1 - f(\mathrm{I}) = b \qquad f(\mathrm{I}) = a + c$$

$$k'_2 = \lambda_2$$

$$k_3 = \lambda_1[c/(a + c)]\Phi_0/\Phi$$

$$k_2 = \lambda_1 - 2k_3$$

From the data reported in Table IV it can be seen that (II) is a minor poorly photoreactive state although (I) leads to both 8-U and 8-C links as well as the product(s) P and is therefore a mixture of conformers designated class I (scheme I).

Nature of Form III tRNA^{Phe} Conformers. In order to define these conformers, our data, i.e., the 8-Pyr cross-links identified here, the kinetic analysis, and the findings that form III tRNA^{Phe} does have extensive secondary structure, should be examined in the light of our knowledge of (i) s^{4}U photochemistry and (ii) alternative secondary structures of tRNA^{Phe}.

s^{4}U is known to photoreact readily and quantitatively with cytidine when the bases are stacked on each other, with the glycosidic bonds antiparallel and the carbon–sulfur bond of s^{4}U parallel to the 5–6 double bond of cytidine, as found in native cross-linkable tRNA (Bergstrom & Leonard, 1972a; Fourrey et al., 1974). In dilute aqueous solution, s^{4}U is readily photooxidized in the presence of free O_2 (Favre, 1974), a photoreaction probably mediated by oxygen species including singlet oxygen (Salet et al., 1985). Finally, when randomly incorporated into single-stranded poly(s^{4}UC), it readily yields intramolecular Pyo(4–5)Cyt links. This cross-linking photoreaction, however, does not occur in a mixture of s^{4}UpC and Cps^{4}U dinucleotides (Favre & Fourrey, 1974). Recently, it was shown that in randomly thiolated oligo(s^{4}UC) the minimal number of residues, N, required to obtain intramolecular cross-linking is $N = 5$ (unpublished data).

Algorithms have been developed [see references in Papanicolaou et al. (1984) and Gouy et al. (1985)] in order to predict the stability order of the various alternative secondary structures derived from the same tRNA sequence. Considering tRNA^{Phe}, the two more stable structures predicted are the cloverleaf (−37.2 kcal/mol) and a long extended structure retaining the CCA and anticodon stems (−35.5 kcal/mol) (Figure 8). Most of the following less stable structures are derived from the latter structure by rearrangement of the base-paired regions distinct from the CCA and anticodon stem (a few variants are shown in Figure 8). In class II conformers (scheme I), s^{4}U cannot yield an intramolecular link and, furthermore, appears weakly reactive. A likely secondary structure that fits these features is the cloverleaf itself. Potentially, cross-linkable pyrimidines would, in this structure, be localized essentially in the variable loop. When the strong electrostatic repulsions between the different bihelical regions are taken into account, it is likely that the CCA and TΨC stems form a continuous helix with the dihydrouracil and anticodon stems oriented roughly perpendicular and in opposite directions, thus maintaining the variable loop extended in a position not accessible to s^{4}U$_8$.

In the major class I tRNA^{Phe} conformers, s^{4}U yields Pyo(4–5)Pyr links with an efficiency 5–6 times lower than in native tRNA^{Phe} [notice that in native tRNA^{Phe}, the 8–13 cross-linking rate is among the slowest found in tRNA species (Favre et al., 1975a)] and, furthermore, is rather susceptible to photooxidation (Scheme I). Hence, in none of these conformers s^{4}U is rigidly held in the appropriate position to yield the Pyo(4–

5)Pyr adduct. Class I secondary structure yielding the 8–(66–68) and the minor 8–(59–62) cross-links can be viewed as a mixture of $tRNA^{Phe}$ conformers in equilibrium on the time scale of the photoreaction as shown in Figure 8. It is more difficult to explain the origin of the 8–(40–43) cross-link on the basis of the extended structure of Figure 8. Folding of these structures to specifically bring the region $\Psi_{39}CCC$ in the vicinity of s^4U_8 appears unlikely in view of the strong electrostatic repulsions involved. We are then led to the possibility of an alternative minor secondary structure retaining the dihydrouracil and TΨC stems, the lower part of the 5′-CCA stem being now paired with the sequence $C_{42}C_{43}G_{44}$. This would bring $C_{40}C_{41}$ in the vicinity of s^4U_8.

One unexpected product of our kinetic studies is that, in form III $tRNA^{Phe}$, two classes of conformers coexist that are not in equilibrium on a relatively long time scale. This situation is not without precedent in the tRNA field since metastable inactive states of yeast $tRNA^{Leu}$ (Gartland & Sueoka, 1966) and *E. coli* $tRNA^{Trp}$ (Lindahl et al., 1966) can occur under conditions that favor the active forms. We interpret this finding as an indication that electrostatic repulsions may maintain as far apart as possible the bihelical regions and prevent major conformational rearrangements between, for example, the cloverleaf and the extended forms of Figure 8. It should be mentioned that the stability prediction would yield more weight to the cloverleaf than observed here. However, these predictions are derived from thermodynamic parameters obtained in medium of moderate ionic strength (Gouy et al., 1985) and do not take into account the electrostatic repulsions prevailing in a low ionic strength medium.

ACKNOWLEDGMENTS

We are indebted to Dr. R. Buckingham for a careful reading of the manuscript as well as to Dr. F. Rodier for his help in the use of the Provencher program. We also thank Drs. Papanicolaou and Gouy, who provided us a list of $tRNA^{Phe}$ alternative secondary structures.

Registry No. s^4U, 13957-31-8; Pdo(4–5)Cyd, 33602-88-9; Pdo(4–5)Urd, 103793-79-9; N_1N_1'-dimethyl-Pyo(4–5)Ura, 103793-77-7; N_1N_1'-dimethyl-Pyo(4–5)hUra, 103793-78-8; N_1N_1'-dimethyl-Pyo(4–5)hCyt, 68455-51-6; N_1N_1'-diriboside Pyo(4–5)hCyt, 103793-76-6.

REFERENCES

Ballini, J. P., Vigny, P., Thomas, G., & Favre, A. (1976) *Photochem. Photobiol. 24*, 321–329.

Bergstrom, D. E., & Leonard, N. J. (1972a) *Biochemistry 11*, 1–8.

Bergstrom, D. E., & Leonard, N. J. (1972b) *J. Am. Chem. Soc. 94*, 6178–6184.

Branch, A. D., Benenfeld, B. J., & Robertson, H. D. (1985) *Nucleic Acids Res. 13*, 4889–4903.

Cole, P. E., Yang, S. R., & Crothers, D. M. (1972) *Biochemistry 11*, 4358–4368.

Favre, A. (1974) *Photochem. Photobiol. 19*, 15–19.

Favre, A., & Yaniv, M. (1971) *FEBS Lett. 17*, 236–240.

Favre, A., & Fourrey, J. L. (1974) *Biochem. Biophys. Res. Commun. 58*, 507–515.

Favre, A., Yaniv, M., & Michelson, A. M. (1969) *Biochem. Biophys. Res. Commun. 37*, 266–271.

Favre, A., Michelson, A. M., & Yaniv, M. (1971) *J. Mol. Biol. 58*, 367–379.

Favre, A., Roques, B., & Fourrey, J. L. (1972) *FEBS Lett. 24*, 209–214.

Favre, A., Buckingham, R., & Thomas, G. (1975a) *Nucleic Acids Res. 2*, 1421–1431.

Favre, A., Morel, C., & Scherrer, K. (1975b) *Eur. J. Biochem. 57*, 147–157.

Favre, A., Ballini, J. P., & Holler, E. (1979) *Biochemistry 18*, 2887–2895.

Fourrey, J. L., Jouin, P., & Moron, J. (1974) *Tetrahedron Lett. 35*, 3005–3006.

Gartland, W. J., & Sueoka, N. (1966) *Proc. Natl. Acad. Sci. U.S.A. 55*, 948–956.

Goldstein, R. N., Stefanovic, S., & Kellenbach, N. R. (1972) *J. Mol. Biol. 69*, 217–236.

Gouy, M., Marliere, P., Papanicolaou, C., & Ninio, J. (1985) *Biochimie 67*, 523–531.

Grabowski, P. J., Padgett, R. A., & Sharp, P. A. (1984) *Cell (Cambridge, Mass.) 37*, 415–427.

Guschlbauer, W., Richards, E. G., Beurling, K., Adams, A., & Fresco, J. (1965) *Biochemistry 4*, 964–975.

Hyde, E. I., & Reid, B. R. (1985a) *Biochemistry 24*, 4307–4314.

Hyde, E. I., & Reid, B. R. (1985b) *Biochemistry 24*, 4315–4325.

Ladner, J. E., Jack, A., Robertus, J. D., Brown, R. S., Rhodes, D., Clarck, B. F. C., & Klug, A. (1975) *Proc. Natl. Acad. Sci. U.S.A. 72*, 4414–4418.

Le Pecq, J. B., & Paoletti, C. (1967) *J. Mol. Biol. 27*, 87–106.

Lindahl, T., Adams, A., & Fresco, J. R. (1966) *Proc. Natl. Acad. Sci. U.S.A. 55*, 941–948.

Ofengand, J., & Bierbaum, J. (1973) *Biochemistry 12*, 1977–1984.

Papanicolaou, C., Gouy, M., & Ninio, J. (1984) *Nucleic Acids Res. 12*, 31–44.

Pearson, R. L., Weiss, J. F., & Kelmers, A. D. (1971) *Biochim. Biophys. Acta 228*, 770–774.

Provencher, S. W. (1976) *Biophys. J. 16*, 27–41.

Quigley, G. J., Wang, A. H. J., Seeman, N. C., Suddath, F., Rich, A., Sussman, J. L., & Kim, S. H. (1975) *Proc. Natl. Acad. Sci. U.S.A. 72*, 4866–4870.

Reid, J. C., & Pratt, A. W. (1960) *Biochem. Biophys. Res. Commun. 3*, 337–342.

Riesner, D., Römer, R., & Maass, G. (1969) *Biochem. Biophys. Res. Commun. 35*, 369–376.

Salet, C., Bazin, M., Moreno, G., & Favre, A. (1985) *Photochem. Photobiol. 41*, 617–619.

Silberklang, M., Gillum, A. M., & RajBhandary, U. L. (1979) *Methods Enzymol. 59*, 58–109.

Thomas, G., & Favre, A. (1977) *C. R. Seances Acad. Sci., Ser. D 284*, 1345–1347.

Thomas, G., Fourrey, J. L., & Favre, A. (1978) *Biochemistry 17*, 4500–4508.

Wollenzien, P. L., & Cantor, C. R. (1982) *J. Mol. Biol. 159*, 151–166.

APPENDIX: COMPUTATION OF THE RADIUS OF GYRATION OF A CLOSED RING TO WHICH LINEAR SIDE CHAINS ARE ATTACHED

We have to compute the radius of gyration, R, of a closed ring of N beads to which linear side chains of I and J beads are attached by their end at the same point of the ring. In a first approach, the chains have the following properties. They follow a Gaussian statistics, whatever their length. They are infinitely thin and can cross one another like phantoms. Under these simplifying hypotheses, our problem can be solved by using the method developed by Zimm and Stockmayer (1949) to determine R in the case of linear molecules containing branches. For our very particular system, we find

$$\langle R^2 \rangle = \frac{b^2}{12}\left[N + 2\frac{(I+J)^2}{t} + 3N\frac{(I-J)^2}{t^2} \right] \quad (1)$$